Bench Testing of New Polarimeter with Silicon Photoelastic Modulator for Short Wavelength FIR Laser

Tsuyoshi AKIYAMA, Kazuo KAWAHATA, Shigeki OKAJIMA[1)], Kazuya NAKAYAMA[1)] and Theodore C. OAKBERG[2)]

National Institute for Fusion Science, 322-6 Oroshi-cho, Toki-shi, Gifu 509-5292, Japan
[1)]*Chubu University, 1200 Matsumoto-cho, Kasugai-shi, Aichi 487-8501, Japan*
[2)]*Hinds Instruments, Inc., 3175 NW Aloclek Drive Hillsboro, Oregon 97124, U.S.A.*

(Received 12 December 2006 / Accepted 11 April 2007)

A short wavelength laser whose wavelength is about 50 μm is preferable for a polarimeter and an interferometer in large fusion devises. This paper reports the development of a polarimeter with a photoelastic modulator (PEM) for a CH_3OD laser (wavelengths of 57.2 and 47.6 μm). The PEM with a high-resistive silicon as a photoelastic element has been newly developed. The transmissivity of the high-resistive silicon is high in a far infrared region. The polarimeter with the Si PEM has been tested and the polarization angle is successfully measured. Noise sources (a multi-reflection of the laser beam in the photoelastic element, a measurement error of amplitude of a detector output and an estimation error of the retardation) of the measured angle are also discussed.

Keywords: polarimeter, CH_3OD laser, photoelastic modulator, high-resistive silicon, AR coating

DOI: 10.1585/pfr.2.S1113

1. Introduction

Measurement of the plasma current profile (or q profile) is indispensable for tokamak operations. The importance is increasing because improved confinement modes are thought to be related to the profile [1]. Similarly, the relationship between a position of an internal transport barrier and rational surfaces is discussing in helical devices [2]. A far infrared (FIR) laser polarimeter, which bases on the Faraday effect, has been used for the current profile measurement in tokamaks [3] and is also planed to installed on ITER [4].

The Faraday rotation angle α in a plasma depends not only on the magnetic filed but also on the electron density as follows;

$$\alpha \propto \lambda^2 \int n_e \boldsymbol{B} \cdot d\boldsymbol{s}, \tag{1}$$

where λ is the wavelength of a probe beam, n_e is the electron density and $\boldsymbol{B}$ is the magnetic field strength. Hence, the electron density profile is necessary to evaluate the distribution of the magnetic field strength. In order to measure the density profile simultaneously, an interferometer is combined with the polarimeter [5,6]. On the other hand, the combination with a polarimeter based on the Cotton-Mouton effect is proposed [7] in order to be free from a fringe jump error, which is a principle problem in an interferometer. However, the coupling of these two effects makes the evaluation of the magnetic field difficult. A short wavelength laser can suppress the fringe jump errors because the beam bending effect in a plasma, which causes the errors, is proportional to λ^2. Therefore, a short wavelength FIR laser, CH_3OD laser (simultaneous oscillation at wavelengths of 57.2 and 47.6 μm) has been developed [8–11] for suppression of the fringe jump errors.

Some measurement methods of the Faraday rotation have been proposed and demonstrated so far. From the viewpoint of maintenance, temporal and angle resolutions and compatibility with the interferometer, a measurement method using photo elastic modulators (PEMs) is appropriate and the feasibilities are demonstrated on JT-60U [12]. The PEM modulates the polarization state of an incident beam periodically by stressing a photoelastic material and then arising time-varying birefringence. So far the application of the PEM is limited to the wavelength shorter than infrared region. In this paper the newly developed PEM for the shorter FIR laser beam and the bench-testing of the polarimeter are reported.

2. Specifications of Si PEM Polarimeter

2.1 Principle of measurement of polarization angle

For the description of the polarization state and the evolution in magnetized plasmas and optical components such as a PEM, Stokes vector $\boldsymbol{s}$ and Mueller matrix M are useful [13]. Figure 1 shows the optical arrangement of the bench-testing of the polarimeter. In Fig. 1 a half-wave plate simulates the Faraday rotation α in a plasma. The Stokes vector of an incident beam to the PEM $\boldsymbol{s}^0$ is described as $(\sin 2\alpha, \cos 2\alpha, 0)$. Muller matrix of the PEM M_{PEM}, which

author's e-mail: takiyama@nifs.ac.jp

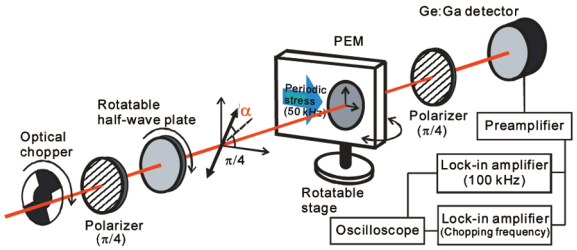

Fig. 1 Optical arrangement for the bench-testing of the polarimeter with a high-resistive Si PEM.

describes changes in the polarization state, is given as follows;

$$M_{\mathrm{PEM}} = \begin{pmatrix} 1 & 0 & 0 \\ 0 & \cos\rho & \sin\rho \\ 0 & -\sin\rho & \cos\rho \end{pmatrix} \quad \rho = \rho_0 \sin(\omega_m t). \tag{2}$$

where ρ is the optical retardation and ω_m is the angle frequency of a piezoelectric transducer to stress the photoelastic element. The Stokes vector $\boldsymbol{s}^1$ after passing through the PEM becomes

$$\begin{aligned} \boldsymbol{s}^1 &= \begin{pmatrix} 1 & 0 & 0 \\ 0 & \cos\rho & \sin\rho \\ 0 & -\sin\rho & \cos\rho \end{pmatrix} \begin{pmatrix} \sin 2\alpha \\ \cos 2\alpha \\ 0 \end{pmatrix} \\ &= \begin{pmatrix} \sin 2\alpha \\ \cos 2\alpha \cos\rho \\ -\cos 2\alpha \sin\rho \end{pmatrix}. \end{aligned} \tag{3}$$

Output signal I of a detector after passing through a polarizer (a transmission angle of $\pi/4$ to the optical axis of the PEM) is as follows.

$$\begin{aligned} I &= \frac{I_0}{2}(1 + s_2^1) \\ &= \frac{I_0}{2}\{1 + \cos 2\alpha \cos(\rho_0 \sin \omega_m t)\} \\ &= \frac{I_0}{2}\left\{1 + J_0(\rho_0)\cos 2\alpha \right. \\ &\quad \left. + 2\cos 2\alpha \sum_{n=1}^{\infty} J_{2n}(\rho_0)\cos(2n\omega_m t)\right\}. \end{aligned} \tag{4}$$

Here, J_k is the Bessel function. Then the polarization angle α can be evaluated from the following formula.

$$\alpha = \frac{1}{2}\cos^{-1}\left(\frac{A}{2J_2(\rho_0) - AJ_0(\rho_0)}\right), \quad A \equiv \frac{I(2\omega_m)}{I(DC)} \tag{5}$$

where A is the ratio of amplitudes of the second harmonic to the DC component of I. The laser beam is chopped with an optical chopper in order to measure the DC component with the use of a lock-in amplifier in the same way as measurement of the second harmonic component.

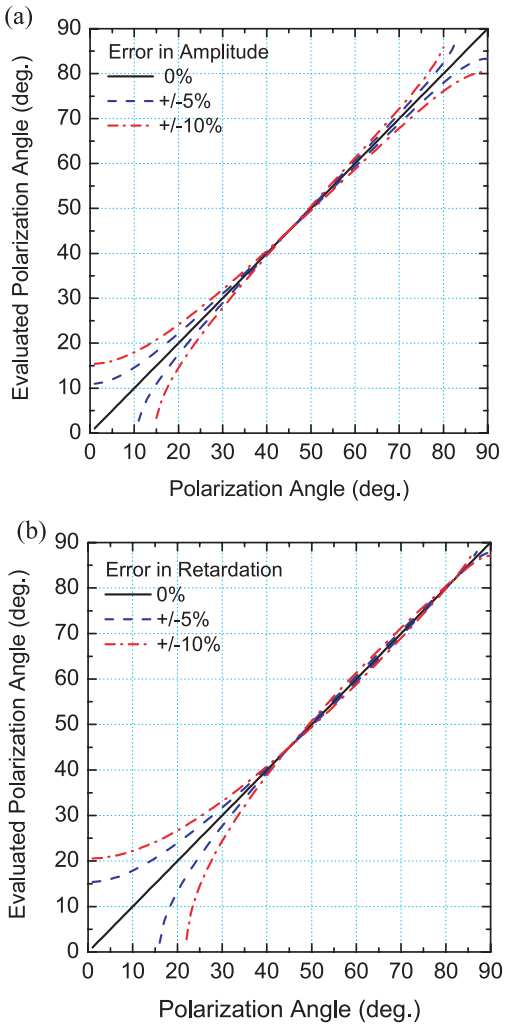

Fig. 2 Effects of error of the measured amplitude (a) and of the retardation (b) on the evaluation of polarization angle.

2.2 Estimation of error terms

Figure 2 (a) shows the evaluated polarization angel from Eq. (5) supposing 0, ±5, and ±10 % measurement errors in the ratio A. The propagation error to the polarization angle becomes large when the polarization angle is near 0 and 90 degrees. The maximum retardation ρ_0 is necessary to evaluate the polarization angle from Eq. (5) and should be measured in advance. The evaluated polarization angle with the error in ρ_0 is shown in Fig. 2 (b). The error in the polarization angle is significant near a polarization angle of 0 degrees. The retardation is determined from both a magnitude of the mechanical stress with the piezoelectric transducer (that is, the applied voltage to the piezoelectric) and the incident angle of a laser beam; changing angle means that the change in the pass length in the photoelastic element. For an in-situ calibration of the retardation, a half wave plate is set to make $\alpha = 0$ where the second harmonic component is maximum. Then, the measured ratio A becomes as follows;

$$A = \frac{2J_2(\rho_0)}{1 + J_0(\rho_0)}. \tag{6}$$

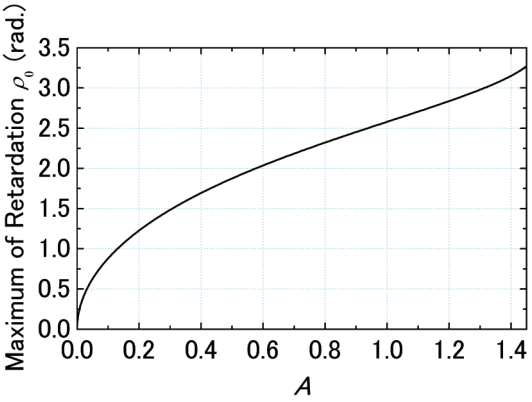

Fig. 3 Relationship between the retardation ρ_0 and the ratio of $2\omega_m$ to DC components A.

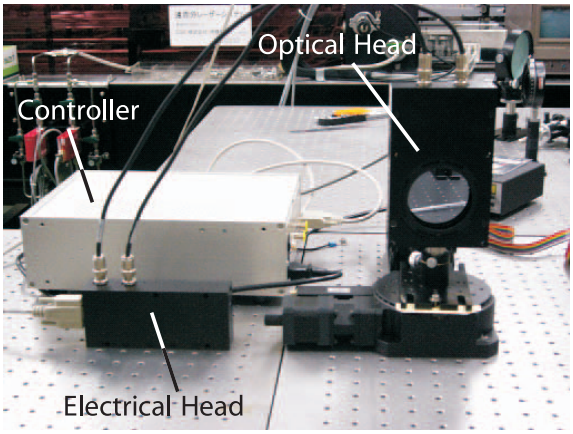

Fig. 4 Photograph of the Si PEM. It consists of the controller, the electrical and the optical head. The optical head is fixed on the rotatable stage.

Since Eq. (6) is a one-valued function of ρ_0 when $\rho_0 < 3.4$ radians (Fig. 3), ρ_0 can be evaluated from Eq. (6).

When a laser is used as a light source, the effect of interference of multi-reflection (because of the high coherence) should be considered. The detected beam intensity I_0 in Eq. (4) is a sum (interference) of the multi-reflected light at the both surfaces of the photoelastic element. A slight change in the thickness of the element due to the periodic stress modulates the interference at the fundamental and the harmonic frequencies. The spurious second harmonic component of the beam intensity I_0, which does not relate to modulations of the polarization, causes the error in the evaluation of the polarization angle and the retardation [14]. Hence, some kinds of technique like an AR coating or adjustment of the incident angle of the beam are necessary to minimize the spurious harmonic component.

2.3 Fabrication of Si PEM

Since there was no PEM for the FIR range so far, we and HINDS instruments, Inc. have developed a new PEM (Fig. 4) with a drive frequency of 50 kHz. As the photoelastic element, it adopts a Si plate with the high resistivity, which has high transmissivity for 57.2 and 47.6 μm [9]. It has not been AR-coated yet. The measured maximum transmissivity in the case of a normal incidence is 50 % and 25 % for 57.2 and 47.6 μm, respectively, because the refractivity is high 3.15 and then the multi-reflection is significant. Hence, the PEM is tilted at several degrees to make the amplitude of the second harmonic component almost zero. Even in such a configuration, the total transmissivity is 50 % and 30 %, respectively. This is because the incident angles where the total intensity and the amplitude of the second harmonic component take external values are different. As the results of the calibration, maximum retardations of 2.7 and 3.0 radians are realized for 57.2 and 47.6 μm, respectively.

3. Experimental Results

The maximum output power of 57.2 and 47.6 μm laser beams are 1.6 and 0.8 W, respectively. Although these two wavelengths oscillate simultaneously, bench-testings of the polarimeter were performed separately; one wavelength can be selected with a polarizer because the polarization angles are perpendicular to each other. The laser beam is chopped with a frequency of 30 Hz. The Faraday rotation is simulated with the half-wave plate made from crystal quartz. A detector is a liquid helium cooled gallium-doped germanium photoconductors (QMC instruments Ltd.). Since Si is not transparent for visible light, beam alignment is carried out with a CW YAG laser beam with a wavelength of 1.06 μm (300 mW, CrystaLaser) superposed to the FIR laser beam. The YAG laser beam can transmit Si and can be visualized easily with an infrared sensor card and an infrared viewer (IRV-1700, Newport).

Figure 5 shows the relationship between the evaluated polarization angle and the actual one estimated from the rotation angle of the half-wave plate in the case of 57.2 μm laser beam. Open circles and triangles show results when the second harmonic component due to the modulation of interference are minimized and are maximized, respectively, by adjusting the incident angle of the laser beam. The adjustment is done without the polarizer to separate modulation components of the interference and the polarization. Error bars show errors of the polarization angle which are attributed to present noises in signal amplitudes (±3 ms with a time constant of 300 ms of lock-in amplifiers), though the data acquisition system has not optimized yet. Good linearity is obtained in a polarization angle smaller than about 70 degrees when the second harmonic component is minimized. The calibrated retardation was 2.27 radians at this condition. However, the reason of the deviation in the case that the polarization angle is larger than 70 degrees has not been clear yet. The small and large deviations in small and large polarization angle, respectively, are not predicted from the error of the signal amplitude and the retardation in Sec. 2.2. When the second harmonic component is maximized, the evaluated angle de-

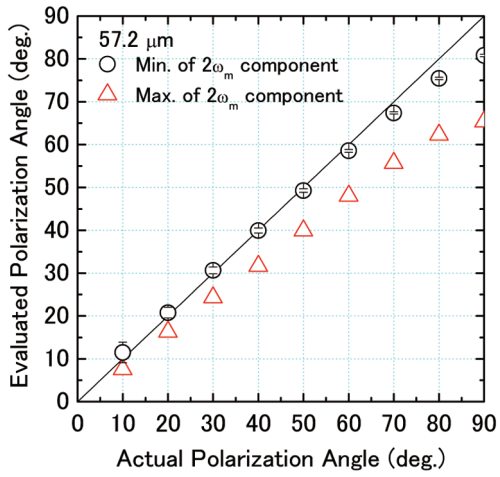

Fig. 5 Relationship between the actual and measured polarization angles.

viates from the actual one. This is because the spurious second harmonic component is added to Eq. (5).

4. Discussion

The reason for the deviation even when the spurious second harmonic component is minimized is speculated as follows. The reflectivities of s- and p-polarization are slightly different. Hence the angle for minimization of the spurious component for one polarization angle is slightly different from that for the orthogonal polarization and then there might be finite spurious components.

Even if the measured polarization angle is deviated from the actual one, we can evaluate the Faraday rotation angle with the use of the calibration curve obtained experiments shown in Sec. 3. However, the reflection, which is the course of the interference, should be reduced as much as possible because a slight change in the incident angle of the beam changes the interference and then the calibration curve becomes different. Hence we have plans of AR-coating of the silicon plate with either Parylene [15] or SiO_2 [16]. With the use of Parylene and SiO_2 film with a thickness of about 8.8 μm (a refractivity N of 1.62 is supposed) and 6.8 μm ($N = 2.10$) will be expected to reduce the reflectivity from 29 % to 2 % for 57.2 μm beam.

The large time constant of our experiment derived from the low frequency of the beam chopping. This can be improved by making up a dual PEMs system [11] with different drive frequencies. We also have a plane to add the second PEM with a drive frequency of 40 kHz.

5. Summary

The Si PEM has been newly developed for a polarimeter using a short wavelength FIR laser, which is suitable for large fusion devices. The polarimeter with the new PEM can measure the polarization angle successfully. The measurement error of amplitude of a detector signal and evaluation error of the retardation results in non-linear errors in evaluated polarization angle. Since a multi-reflection in the photoelastic element also causes the deviation from an actual polarization angle, it should be suppressed by tilting the PEM or an AR-coating.

Acknowledgements

The authors acknowledge Dr. Kawano of Japan Atomic Energy Agency for his valuable comments on PEMs. The authors thank Dr. I. Hosako of the National Institute of Information and Communications Technology for his fruitful advices on the AR-coating in the terahertz region. This work was supported by funds of Grant-in-Aid for Scientific Research on the Priority Area “Advanced Diagnostics for Burning Plasmas” (16082208).

[1] S. Ide, J. Plasma Fusion Research SERIES, **4**, 99 (2001).
[2] T. Shimozuma *et al.*, Nucl. Fusion **45**, 1396 (2005).
[3] H. Soltwisch, Plasma Phys. Contr. Fusion **34**, 1669 (1992).
[4] A.J.H. Donné *et al.*, Rev. Sci. Instrum. **75**, 4694 (2004).
[5] H. Soltwisch, Rev. Sci. Instrum. **57**, 1939 (1986).
[6] J.H. Rommers, J. Howard, Plasma Phys. Control. Fusion **38**, 1805 (1996).
[7] L. Guidicottie *et al.*, Plasma Phys. Control. Fusion **46**, 681 (2004).
[8] S. Okajima *et al.*, Rev. Sci. Instrum **72**, 1094 (2001).
[9] K. Nakayama *et al.*, Rev. Sci. Instrum **75**, 329 (2004).
[10] K. Kawahata *et al.*, Rev. Sci. Instrum **75**, 3508 (2004).
[11] K. Kawahata *et al.*, Rev. Sci. Instrum **77**, 10F132-1 (2006).
[12] Y. Kawano *et al.*, Rev. Sci. Instrum **72**, 1068 (2001).
[13] S.E. Segre, Plasma Phys. Controlled Fusion **41**, R57 (1999).
[14] T.C. Oakberg, Opt. Eng. **34**, 1545 (1995).
[15] A.J. Gatesman *et al.*, IEEE Microwave and Guided Wave Letters **10**, (2006).
[16] I. Hosako, Journal of the National Institute of Information and Communications Technology **51**, 1/2 (2004).